American Mineralogist, Volume 68, pages 1089–1094, 1983

Phase relations in the join kirschsteinite ($CaFeSiO_4$)–fayalite (Fe_2SiO_4)

DILIP K. MUKHOPADHYAY AND DONALD H. LINDSLEY

Department of Earth and Space Sciences
State University of New York, Stony Brook, New York 11794

Abstract

Reversed experiments (P_{H_2O} = 1 kbar; Co–CoO or WM buffer) on the kirschsteinite ($CaFeSiO_4$)–fayalite (Fe_2SiO_2) join outline a miscibility gap below approximately 1041°C. Experimental results are compatible with a simple, symmetric Margules model having W_G of 21866±143 J. We treat kirschsteinite as an end-member with the implicit assumption that Ca–Fe mixing occurs only in M2 site of the olivine structure. Evidence has been adduced to show that olivines with more Ca_2SiO_4 component than in $CaFeSiO_4$ can occur, but for those olivines there appears to be a strong partitioning of Ca into M2 site; thus kirschsteinite may serve as an effective end-member. Least-squares refinement of unit-cell parameters show that all three cell edges and the unit-cell volume vary linearly with composition in fayalite–kirschsteinite olivines. Based on the experimental data of Bowen *et al.* (1933) and an assumption of ideality in the liquid, the enthalpy of melting of kirschsteinite has been estimated at 106.1±10.6 kJ. The melting relations of fayalite–kirschsteinite olivines that have been calculated show some discrepancy with the experimental determination of Bowen *et al.* (1933).

Introduction

The Ca–Mg–Fe^{2+} olivines can be adequately represented on an olivine quadrilateral with the end-members forsterite (Mg_2SiO_4), fayalite (Fe_2SiO_4), kirschsteinite ($CaFeSiO_4$), and monticellite ($CaMgSiO_4$). Among the four binary series between the end-members of the olivine quadrilateral, the forsterite–fayalite series has been most extensively studied because the compositions of most naturally occurring olivines plot very close to the forsterite–fayalite join with less than 1–2 wt.% CaO (Simkin and Smith, 1970). The Ca-bearing parts of the system have not been subjected to as much rigorous experimental investigation, although Ca-rich olivines have been reported by a few authors; Dodd (1971) reported high-Ca olivine from Sharps chondrite, and a Mg-rich kirschsteinite has been described from a complex melilite–nephelinite lava from Belgian Congo by Sahama and Hytönen (1957).

The monticellite–forsterite join has been investigated by Biggar and O'Hara (1969) and Warner and Luth (1973) and others. Warner and Luth have shown that the miscibility gap in the subsolidus region in this system is simple and symmetric. The maximum amount of the $CaMgSiO_4$ component which may be dissolved in the forsteritic olivine is less than 5 mole% under physico-chemical conditions likely to exist in the natural systems.

The experimental investigations by Bowen *et al.* (1933) in the Ca_2SiO_4–Fe_2SiO_4 system show that there is a minimum in the melting curve between $CaFeSiO_4$ and Fe_2SiO_4 (Fig. 1). This indicates that there should be a miscibility gap in the subsolidus region in this system. The disparity in the six-coordinated ionic radii between Ca and Fe^{2+} (1.00Å and 0.72Å, respectively; Shannon and Prewitt, 1969) also supports this view. For these reasons the kirschsteinite–fayalite series has been chosen for experimental investigation to search for and map accurately the subsolidus two-phase region. The experimental data then may be used through suitable solution models to retrieve important thermochemical quantities (Thompson, 1967; Saxena, 1972). This would help us in modelling the olivine quadrilateral and also in modelling Fe^{2+}-rich pyroxenes (see Lindsley, 1981).

Experimental details

Syntheses of starting materials

The end-members fayalite (Fa_{100}) and kirschsteinite (Kst_{100}) and intermediate compositions $Fa_{25}Kst_{75}$, $Fa_{50}Kst_{50}$, and $Fa_{75}Kst_{25}$ (in mole percent) were synthesized from carefully weighed and ground (in agate mortar) oxide mixes. The fayalite was synthesized in an Fe-saturated platinum crucible at about 1100°C for about four hours in a CO–CO_2 atmosphere maintained at fO_2 in the fayalite field. The kirschsteinite mix was wrapped in silver foil and sealed in an evacuated silica glass tube and was run at 940°C for about 360 hours. This partly reacted material was then run at 800°C and 1 kbar pressure (with WM buffer) for 22 hours to complete the reaction. The mixes with intermediate compositions were loaded in reduced Fe capsules, sealed in evacuated silica glass tubes, and reacted at about 1100°C. Two other phases with excess Ca_2SiO_4 (larnite) component relative to

0003–004X/83/1112–1089$02.00

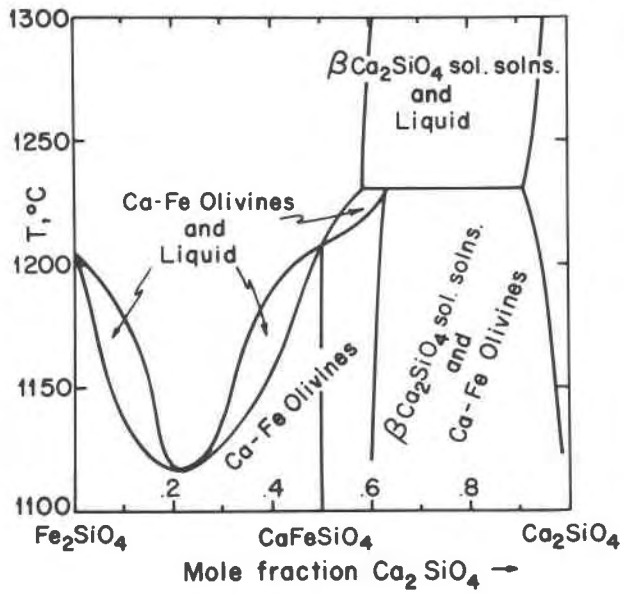

Fig. 1. The system Ca_2SiO_4–Fe_2SiO_4 (after Bowen *et al.*, 1933), converted to mole%.

$CaFeSiO_4$ were also synthesized. These phases ($Fa_{45}La_{55}$ and $Fa_{40}La_{60}$) were synthesized in the same way as the intermediate compositions but were reacted at 1168°C for about 333 hours. A summary of the experimental conditions is given in Table 1.

Two-phase determination

Synthesized single phase $Fa_{50}Kst_{50}$ and homogeneous 50:50 mechanical mixtures between synthetic fayalite and kirschsteinite were used as starting materials, in order to bracket the compositions of the equilibrium reactions. A summary of the experimental conditions is given in Table 2. For the 1 kbar experiments, charges were loaded with about 5–8 wt.% H_2O in $Ag_{80}Pd_{20}$ capsules and enclosed with Co–CoO or WM buffer (charges oxidized at FMQ buffer) with H_2O in Au capsules according to methods described by Huebner (1971). The experiments at 750°, 800°, 850°, and 900°C were carried out in standard cold seal pressure vessels with CH_4 gas as a pressure medium. For the experiments at 940°, 1000°, and 1040°C, the charges were loaded in Fe capsules, sealed in evacuated silica glass tubes, and run in a quench furnace. The accuracy of temperature and pressure are believed to be ±5°C and ±20 bars for the hydrothermal runs and ±3°C for the runs in evacuated silica glass tubes.

Table 1. Olivine syntheses data

Starting material composition	Run conditions	Time (hrs)	Result
Kst_{100}	940°, vacuum +	360 +	Kst
	800°, 1 kb, WM buffer	22	
Fa_{100}	1100°, 1 atm (CO-CO_2)	∿ 4	Fa
$Fa_{50}Kst_{50}$	1100°, vacuum	281 + 144	Ol_{ss}
$Fa_{25}Kst_{75}$	996°, vacuum	96	Ol_{ss}
$Fa_{75}Kst_{25}$	996°, vacuum	96	Ol_{ss}
$Fa_{45}La_{55}$	1168°, vacuum	333	Ol_{ss}*
$Fa_{40}La_{80}$	1168°, vacuum	333	Ol_{ss}

Microprobe analysis gives a composition of $Fa_{44}La_{56}$ (see Fig. 2).

Table 2. Experimental results

Run No.	Starting Material	T°C	PKb	Buffer	X-Ray Data* Kst_{ss} X_{Kst}	X-Ray Data* Fa_{ss} X_{Fa}	Microprobe* Kst_{ss} X_{Kst}	Microprobe* Fa_{ss} X_{Fa}
1	MM	750	1	CoCoO	88.5	88	83	85.5
2	1Ph	750	1	CoCoO	86.5	81	85	89
3	MM	800	1	WM	84.5	89.5	85	85.5
4	1Ph	800	1	WM	85.5	88	82	87.5
5	MM	850	1	WM	83	82.5	83	82
6	1Ph	850	1	WM	81.5	82.5	84.5	82
7	MM	900	1	WM	80	81	79	77
8	1Ph	900	1	WM	74.5	78	79	78.5
9	MM	940	Vacuum	---	74.5	67.5	75	69.5
10	1Ph	940	Vacuum	---	75	70	52	53
11	MM	1000	Vacuum	---	73	76.5	56	57.5
12	1Ph	1000	Vacuum	---	---	---	---	---
13	MM	1040	Vacuum	---	$Fa_{46}Kst_{54}$		$Fa_{46}Kst_{54}$	
14	1Ph	1040	Vacuum	---	$Fa_{48}Kst_{52}$		$Fa_{48}Kst_{52}$	

MM: 50:50 mechanical mixture between fayalite and kirschsteinite.
1Ph: Homogeneous single phase $Fa_{50}Kst_{50}$.
**: In mole percent.*

Analytical techniques

All the charges were examined in oil mounts under petrographic microscope and by powder X-ray diffraction to check for homogeneity and completeness of reaction. A determinative curve for composition was prepared from the X-ray diffraction patterns of the synthetic single phases for rapid determination of the composition of the experimental products. The (130) peak was chosen because it is one of the strongest olivine peaks and lies very close to one of the peaks of the internal standard, CaF_2, used. The compositions of the charges of both synthesis and two-phase determination experiments were also checked by electron microprobe analysis (ARL-EMX-SM, 4-spectrometer, with on line data reduction technique of Bence–Albee and Albee–Ray). An accelerating potential of 15 kV and a specimen current of 0.015 μA on brass were used. Rockport fayalite, diopside, and synthetic single phase $Fa_{50}Kst_{50}$ served as standards. Only those analyses with oxide sums of 100±2 wt.% and cation sums of 3.00±0.02 per four oxygens were accepted; most of the analyses fell within these ranges.

Lumpkin *et al.* (1983) have shown that d_{130} varies with cation ordering as well as with bulk composition in Ca–Mg olivines, and the same may well be true for Ca–Fe olivines. However, the effect is relatively small, and is not expected to be important in the present case for the following reasons: (1) In our experiments at relatively low temperatures (750–900°C), where ordering might be expected to be maximized, there is excellent agreement between compositions determined from *d*-spacing and by microprobe. (2) At the higher temperatures where X-ray and microprobe compositions are in serious disagreement because of fine grain size, the temperatures approach those at which the X-ray standards were synthesized, and thus the degrees of ordering should be similar.

Results

Results of least-squares refinement of unit-cell parameters from the X-ray diffraction patterns of the synthetic single-phase starting materials are given in Table 3 and plotted in Figure 2. In accord with the results of Wydenko and Mazanek (1968), all three cell edges and the unit-cell

Table 3. Unit-cell dimensions of synthetic Ca–Fe^{2+} olivines

Composition	a(Å)	b(Å)	c(Å)	V(Å^3)	No. of lines used for refinement
Fa_{100}	4.815 ± 0.007	10.49 ± 0.01	6.087 ± 0.009	307.6 ± 0.5	8
$Fa_{75}Kst_{25}$	4.829 ± 0.008	10.679 ± 0.009	6.167 ± 0.006	318.0 ± 0.4	7
$Fa_{50}Kst_{50}$	4.851 ± 0.009	10.818 ± 0.007	6.236 ± 0.009	327.3 ± 0.4	10
$Fa_{25}Kst_{75}$	4.866 ± 0.009	11.00 ± 0.01	6.347 ± 0.008	339.7 ± 0.5	27
Kst_{100}	4.865 ± 0.002	11.147 ± 0.002	6.432 ± 0.002	348.8 ± 0.1	9
$Fa_{45}La_{55}$	4.896 ± 0.003	11.191 ± 0.005	6.464 ± 0.004	354.2 ± 0.2	14
$Fa_{40}La_{60}$	4.915 ± 0.002	11.199 ± 0.006	6.485 ± 0.002	357.0 ± 0.2	21

volume vary linearly with composition between fayalite and kirschsteinite. Figure 2 shows that the increase in unit-cell volume with increase in Ca is mainly produced by the *b* cell edge. The *c* cell edge moderately affects the unit-cell volume whereas *a* cell edge has only a negligible effect. It is interesting to note that Warner and Luth (1973) found a similar relationship with Ca–Mg olivines, but they reported a slight negative volume of mixing at the forsteritic end-member and no volume of mixing at the $CaMgSiO_4$ end. The unit-cell refinements of the phases with excess Ca_2SiO_4 over $CaFeSiO_4$ show that the unit-cell volume remains linear, whereas *b* cell edge deviates considerably from linearity. Single-crystal X-ray studies of the phase with 60 mole% Ca_2SiO_4 show that the phase is orthorhombic with probable space group similar to olivine.

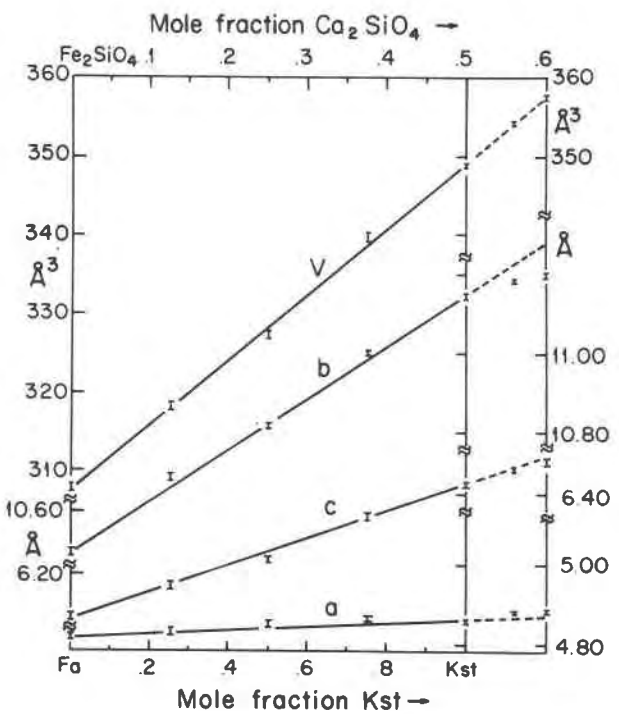

Fig. 2. The variation in unit-cell edges *a*, *b*, and *c* and unit-cell volume (*V*) with composition in synthetic Ca–Fe^{2+} olivines. Data from Table 2.

The compositions of the coexisting olivines were determined from the X-ray determinative curve and by microprobe analysis (see Table 2). The experimental results are shown in Figure 3. The compositions determined by the two methods are compatible with each other up to 900°C. Moreover, the compositions for each pair of starting phases are nearly identical, indicating equilibrium reactions. However, above 900°C the two methods yield different apparent compositions. The high-temperature experiments produced very fine-grained charges that could not be resolved satisfactorily by microprobe analysis. The X-ray data show that at 940°C the single phase unmixed considerably, although unmixing was undetected in the probe data. Similarly at 1000°C the two types of data are not compatible with each other. At high-temperatures the exsolving reaction is very sluggish, because as the miscibility gap narrows down the free energy of reaction becomes very small. At 1040°C the mechanical mixture homogenized completely, whereas the single phase did not unmix at all.

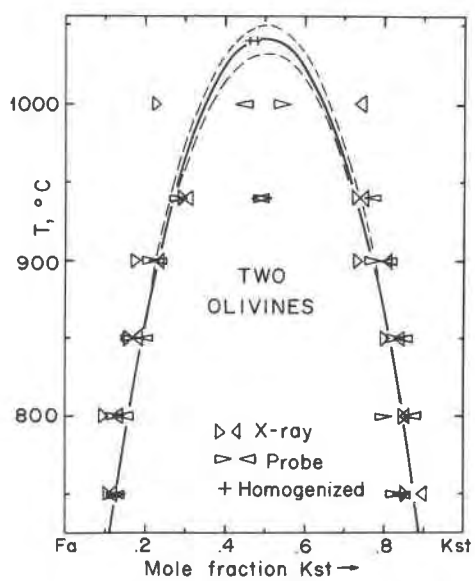

Fig. 3. The experimental results (data given in Table 2) and the calculated miscibility gap in the fayalite–kirschsteinite series with W_G = 21866 J. The effect of uncertainty in W_G on the calculated miscibility gap is shown by dashed lines.

Discussion

A visual inspection of the experimental data (Fig. 3) show that the miscibility gap is approximately symmetric. The experimental data, however, can only bracket the composition of the coexisting olivines, and we have ranges of compositions of olivines at each temperature. To solve this problem, numerical analyses of the experimental data were carried out following the methods described by Thompson (1967).

At equilibrium (Equation 58, Thompson, 1967) (subscripts indicate components, superscripts indicate phases):

$$\mu_{Fa}^{Fa_{ss}} = \mu_{Fa}^{Kst_{ss}} \text{ and } \mu_{Kst}^{Fa_{ss}} = \mu_{Kst}^{Kst_{ss}}$$

or

$$\alpha RT \ln X_{Fa}^{Fa_{ss}} + (X_{Kst}^{Fa_{ss}})^2 W_G = \alpha RT \ln X_{Fa}^{Kst_{ss}} + (X_{Kst}^{Kst_{ss}})^2 W_G$$

and

$$\alpha RT \ln X_{Kst}^{Fa_{ss}} + (X_{Fa}^{Fa_{ss}})^2 W_G = \alpha RT X_{Kst}^{Kst_{ss}} + (X_{Fa}^{Kst_{ss}})^2 W_G$$

Rearranging,

$$W_G[(X_{Kst}^{Fa_{ss}})^2 - (X_{Kst}^{Kst_{ss}})^2] = \alpha RT \ln(X_{Fa}^{Kst_{ss}}/X_{Fa}^{Fa_{ss}})$$

and

$$W_G[(X_{Fa}^{Fa_{ss}})^2 - (X_{Fa}^{Kst_{ss}})^2] = \alpha RT \ln(X_{Kst}^{Kst_{ss}}/X_{Kst}^{Fa_{ss}}),$$

where the μ's are the chemical potentials and the X's are the mole fractions of the components in the solid solutions; α is the dimensionless site-mixing parameter (see below), and W_G is the adjustable Margules parameter.

The least-squares fit of the calculated excess parameter, W_G, from the experimental data shows that the data are compatible with a simple, symmetric Margules model having W_G of 21866 J with an estimated uncertainty of 143 J. The calculated miscibility gap using this W_G value is shown in Figure 3. The solvi bounding the two-phase region disappear at about 1041°C (consolute point). The calculated miscibility gap is remarkably consistent with the experimental data. The experiments run at 1040°C show that the 50:50 mechanical mixture between the end-members completely homogenized, whereas the homogeneous single phase, $Fa_{50}Kst_{50}$, did not unmix at all. The effect of uncertainty in W_G on the calculated miscibility gap is also shown in Figure 3. The uncertainty in the consolute temperature is only ±8°C.

It is very important for this kind of numerical analysis to evaluate the dimensionless term α very carefully (Thompson, 1967). Kirschsteinite has been treated as an end-member with the implicit assumption that Ca enters only in the M2 site of the olivine structure (Onken, 1965). The value of the site mixing parameter, α, has, therefore, been taken as unity. The evidence regarding this assumption is mixed. Bowen *et al.* (1933) show that $CaFeSiO_4$ melts at a single temperature (see Fig. 1), consistent with its being an end-member compound, but they also show a field of "Ca–Fe olivines" extending past $CaFeSiO_4$ to approximately $Fa_{40}La_{60}$ (mole%). But both the refractive indices (Bowen *et al.*, 1933) and the unit-cell parameters (Wyderko and Mazanek, 1968) of these "olivines" show sharp inflections at $CaFeSiO_4$, suggesting an abrupt change in properties at that composition. As mentioned earlier, we have synthesized phases with excess Ca_2SiO_4 ($Fa_{45}La_{55}$ and $Fa_{40}La_{60}$) and find that their powder X-ray diffraction patterns are completely compatible with olivine structure. Single-crystal X-ray diffraction patterns of $Fa_{40}La_{60}$ strongly suggest that this phase is orthorhombic with space group *Pbnm* (or *Pnma,* depending on the choice of the unit cell). Furthermore, in contrast with the results of Wyderko and Mazanek, we find that the unit-cell parameters, except *b* cell edge, form a linear extension of the values determined for Fa–Kst olivines. Our Ca-rich olivines were synthesized at 1165–1170°C; those of Wyderko and Mazanek were reported as formed "above the melting point", the implication being that their data pertain either to quench-crystals or to materials annealed at unspecified subsolidus temperatures.

Lumpkin *et al.* (1983) reported that the Ca-Mg olivines synthesized by Warner and Luth (1973) are "highly ordered:" more than 80% of the Ca occurs in the M2 site in Fo-rich olivines with more than 95% in M2 for the $CaMgSiO_4$-rich olivines.

Thus, the preponderance of evidence suggests that Ca–Fe olivines with more than 50 mole% Ca_2SiO_4 can exist, and, perforce, some Ca must enter the M1 site. But there appears to be a strong partitioning of Ca into the M2 site and, thus, $CaFeSiO_4$ appears to serve as an effective end-member. It may be possible that so long as M2 sites are available Ca is strongly partitioned into M2 sites of the olivine structure and once all the M2 sites are occupied, then Ca replaces Fe in the M1 sites also. This may be due to the fact that the M2 sites in olivine are larger than the M1 sites (Birle *et al.*, 1968). As Ca starts entering M1 sites, the *b* cell edge is possibly not as strongly affected, causing its deviation from linearity with composition (see Fig. 2). Accordingly, we have adopted the site mixing parameter, α, as unity and neglected any effects of intrasite partitioning. The remarkable comparability between the experimental data and the calculated miscibility gap suggests that the model is useful even if not rigorously correct.

We used the 2 kbar data on the monticellite–forsterite join from Warner and Luth (1973) and fitted them with a temperature independent, symmetric Margules model, obtaining an excess parameter, W_G, of 33922 J, with an estimated uncertainty of 116 J. The W_G's of these two systems may be compared with each other because the unit-cell volume in the fayalite–kirschsteinite join varies linearly with composition, indicating that the limits of miscibility are independent of pressure in this system. The excess parameter in the Fe-free system is approximately 12 kJ larger than that for the Mg-free olivines. For comparison, the differences in the (asymmetric) Margules parameters determined for Ca–Mg clinopyroxenes

(Lindsley *et al.*, 1981) and Ca–Fe clinopyroxenes (Lindsley, 1981) are approximately 8–10 kJ.

The melting relations of fayalite–kirschsteinite olivines as given by Bowen *et al.* (1933) are solely dependent on a few experimental points (see Fig. 1). We have calculated the liquidus and the solidus curves between fayalite and kirschsteinite following methods described below.

Assuming $\Delta C_P = 0$ we can write (Carmichael *et al.*, 1974, p. 172),

$$\ln a^{liq}_{Kst} - \ln a^{ss}_{Kst} = \frac{(\Delta H^{Kst}_m)_{Tm}}{R}\left(\frac{1}{T^{Kst}_m} - \frac{1}{T}\right)$$

where ΔH^{Kst}_m is enthalpy of melting of kirschsteinite, a's are the respective activities, T^{Kst}_m is temperature of melting of kirschsteinite, and T is the temperature of experiment.

Assuming the liquid to be ideal, replacing appropriate terms for activity of solid solution (Thompson, 1967), and rearranging terms we get,

$$(\Delta H^{Kst}_m)_{Tm} = \frac{[\ln X^{liq}_{Kst} - \ln X^{ss}_{Kst} - (1 - X^{ss}_{Kst})^2 W_G/RT]R}{(1/T^{Kst}_m - 1/T)}$$

Least-squares fit of the experimental data of Bowen *et al.* yields an enthalpy of melting of kirschsteinite of 106.1 kJ with an estimated uncertainty of 10.6 kJ. Fayalite and kirschsteinite melt congruently at 1205° and 1208°C, respectively, and Robie *et al.* (1978) give enthalpy of melting of fayalite as 92.173 kJ. Correspondingly, the entropies of melting of these two end-members are 62.357 J and 71.657 J, respectively. Using these data we can calculate the solidus and liquidus curves for fayalite–kirschsteinite olivines (Thompson, 1967).

At equilibrium,

$$\mu^{liq}_{Fa} = \mu^{ss}_{Fa} \quad (1)$$

and

$$\mu^{liq}_{Kst} = \mu^{ss}_{Kst} \quad (2)$$

Expanding Equation (1) and taking $\alpha = 1$ we get,

$$\Delta\overline{G}_{Fa,T} + RT \ln X^{liq}_{Fa} = RT \ln X^{ss}_{Fa} + (1 - X^{ss}_{Fa})^2 W_G$$

or

$$X^{liq}_{Fa} = \exp\left[\frac{RT \ln X^{ss}_{Fa} + (1 - X^{ss}_{Fa})W_G - \Delta\overline{G}_{Fa,T}}{RT}\right] \quad (3)$$

where

$$\Delta\overline{G}_{Fa,T} = \mu^{o,liq}_{Fa} - \mu^{o,ss}_{Fa} = \Delta H^{Fa}_m - T\Delta S^{Fa}_m$$

at temperature T, assuming $\Delta C_P = 0$.

Expanding Equation (2) in similar way we get,

$$\Delta\overline{G}_{Kst,T} + RT \ln(1 - X^{liq}_{Fa}) = RT \ln(1 - X^{ss}_{Fa}) + (X^{ss}_{Fa})^2 W_G \quad (4)$$

where

$$\Delta\overline{G}_{Kst,T} = \mu^{o,liq}_{Kst} - \mu^{o,ss}_{Kst} = \Delta H^{Kst}_m - T\Delta S^{Kst}_m$$

at temperature T, assuming $\Delta C_P = 0$.

Substituting Equation (3) in Equation (4) and rearranging terms,

$$RT \ln\left[1 - \exp\left(\frac{RT \ln X^{ss}_{Fa} + (1 - X^{ss}_{Fa})^2 W_G - \Delta\overline{G}_{Fa,T}}{RT}\right)\right] - RT \ln(1 - X^{ss}_{Fa}) + (X^{ss}_{Fa})^2 W_G - \Delta\overline{G}_{Kst,T} = 0 \quad (5)$$

Equation (5) cannot be solved by simple algebraic methods because it has become transcendental. However, at any temperature X^{ss}_{Fa} can be calculated very quickly by successive iteration. X^{liq}_{Fa} then may be easily calculated using equation (3). This method of calculation for the composition of coexisting liquid and solid solution is very precise and simple if a computer is used.

The calculated melting relations of fayalite–kirschsteinite olivines are shown in Figure 4, together with the experimental data points of Bowen *et al.* (1933), for comparison. The match between the calculated and experimental data is good except at $X_{Kst} = 0.75$. The disagreement there is probably due to some combination of the following: nonideality of the liquid, nonsymmetrical excess free energy of the olivine, nonzero values of ΔC_P, or experimental uncertainties in the data of Bowen *et al.* (1933).

The shape of the azeotrope in Figure 4, especially the nearly isothermal solidus for $0.4 \leq X \geq 0.6$, is different

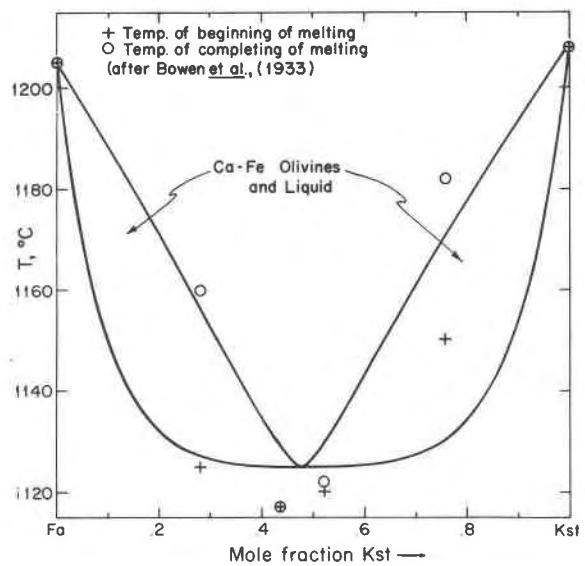

Fig. 4. Calculated melting relations in the fayalite–kirschsteinite series. Experimental data of Bowen *et al.* (1933) are also shown.

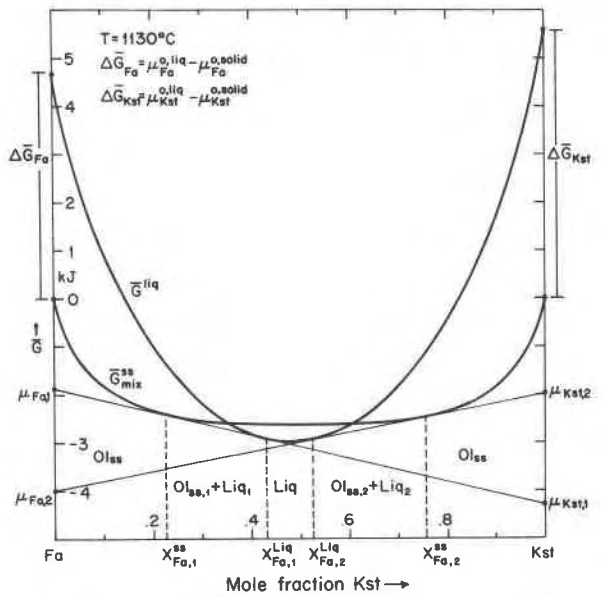

Fig. 5. Calculated $\overline{G}$–X curves for Ca–Fe olivines and liquid at 1130°C.

from the way such diagrams are usually sketched, but is required by the model and assumptions we use. The nearly isothermal solidus is a consequence of the shape of the G-curve for olivine (Fig. 5); it "anticipates" the consolute point of the two-olivine field that lies some 80°C below.

The present work constitutes part of a continuing experimental investigation on the Ca-bearing parts of the olivine quadrilateral. As more phase equilibrium data become available, we will be able to calculate an olivine solution model. This model would also help us in calculating Hd_{ss}–Ol–Qtz equilibria for high Fe/(Fe+Mg) using solution models presented by Lindsley (1981).

Acknowledgments

The authors wish to acknowledge critical reviews by R. Reeder, S. K. Saxena and J. Longhi. This work was supported by NSF Grant #EAR80-25260.

References

Biggar, G. M., and O'Hara, M. J. (1969) Monticellite and kirschsteinite crystalline solutions. Journal of the American Ceramic Society, 52, 249–252.

Birle, J. D., Gibbs, G. V., Moore, P. B., and Smith, J. V. (1968) Crystal structures of natural olivines. American Mineralogist, 53, 807–824.

Bowen, N. L., Schairer, J. F., and Posnjak, E. (1933) The system Ca_2SiO_4–Fe_2SiO_4. American Journal of Science, 26, 273–297.

Carmichael, I. S. E., Turner, F. J., Verhoogen, J. (1974) Igneous Petrology. McGraw-Hill, New York.

Dodd, R. T. (1971) Calc–aluminous insets in olivine of the Sharps chondrite. Mineralogical Magazine, 38, 451–458.

Huebner, J. S. (1971) Buffering techniques for hydrostatic systems at elevated pressures. In G. C. Ulmer, Ed., Research Techniques for High Pressure and Temperature, p. 123–177. Springer-Verlag, New York.

Lindsley, D. H. (1981) The formation of pigeonite on the join hedenbergite–ferrosilite at 11.5 and 15 kbar; Experiments and a solution model. American Mineralogist, 66, 1175–1182.

Lindsley, D. H., Grover, J. E., and Davidson, P. M. (1981) The thermodynamics of the $Mg_2Si_2O_6$–$CaMgSi_2O_6$ join: A review and an improved model. In R. C. Newton, A. Navrotsky, and B. J. Wood, Eds., Advances in Physical Chemistry, Vol. 1, p. 149–175. Springer-Verlag, New York.

Lumpkin, G. R., Ribbe, P. E., and Lumpkin, N. E. (1983) Composition, order–disorder and lattice parameters of olivines: Determinative methods for Mg–Mn and Mg–Ca silicate olivines. American Mineralogist, 68, 1174–1182.

Onken, H. (1965) Verfeinerung der Kristllastruktur von Monticellit. Tschermak's Mineralogische und Petrographische Mitteilungen, 10, 34–44.

Robie, R. A., Hemingway, B. S., and Fisher, J. R. (1978) Thermodynamic properties of minerals and related substances at 298.15 K and 1 bar (10^5 pascals) pressure and at high temperatures. Bulletin U.S. Geological Survey, 1452, 1–456.

Sahama, Th. G., and Hytönen, K. (1957) Kirschsteinite, a natural analog of synthetic iron monticellite, from Belgian Congo. Mineralogical Magazine, 31, 698–699.

Saxena, S. K. (1972) Retrieval of thermodynamic data from a study of intercrystalline and intracrystalline ion exchange equilibrium. American Mineralogist, 57, 1782–1800.

Shannon, R. D., and Prewitt, C. T. (1969) Effective ionic radii in oxides and fluorides. Acta Crystallographica 25, 925–946.

Simkin, T., and Smith, J. V. (1970) Minor-element distribution in olivine. Journal of Geology, 78, 304–325.

Thompson, J. B., Jr. (1967) Thermodynamic properties of simple solutions. In P. H. Abelson, Ed., Researches in Geochemistry, Vol. 2, p. 340–361. John Wiley and Sons, New York.

Warner, R. D., and Luth, W. C. (1973) Two-phase data for the join monticellite ($CaMgSiO_4$)–forsterite (Mg_2SiO_4): Experimental results and numerical analysis. American Mineralogist, 58, 998–1008.

Wyderko, M., and Mazanek, E. (1968) The mineral characteristics Ca–Fe olivine. Mineralogical Magazine, 36, 955–961.

Manuscript received, April 2, 1982;
accepted for publication, April 18, 1983.